
EFDA–JET–CP(04)01/18

E. de la Luna, G. Conway, J. Fessey, R. Prentice, D.V. Bartlett, J. M. Chareau,
C. Gowers, J. Sánchez, W. Suttrop, V. Tribaldos and JET-EFDA contributors.

Electron Cyclotron Emission Radiometer Upgrade on the JET Tokamak

Electron Cyclotron Emission Radiometer Upgrade on the JET Tokamak

E. de la Luna¹, G. Conway², J. Fessey³, R. Prentice³, D.V. Bartlett⁵,
J. M. Chareau⁴, C. Gowers³, J. Sánchez¹, W. Suttrop², V. Tribaldos¹
and JET-EFDA contributors*

¹*Asociación EURATOM-CIEMAT para Fusión, CIEMAT, Madrid, Spain*

²*IPP-EURATOM Association, Garching, Germany*

³*EURATOM-UKAEA Fusion Associations, Culham Science Centre, Abingdon, UK*

⁴*European Commission, Institute for Transuranium Elements, Karlsruhe, Germany*

⁵*European Commission, DG Research J.6, Brussels, Belgium*

* See annex of J. Pamela et al, "Overview of Recent JET Results and Future Perspectives",
Fusion Energy 2000 (Proc. 18th Int. Conf. Sorrento, 2000), IAEA, Vienna (2001).

Preprint of Paper to be submitted for publication in Proceedings of the
15th HTPD Conference,
(San Diego California, USA 18-22 April 2004)

“This document is intended for publication in the open literature. It is made available on the understanding that it may not be further circulated and extracts or references may not be published prior to publication of the original when applicable, or without the consent of the Publications Officer, EFDA, Culham Science Centre, Abingdon, Oxon, OX14 3DB, UK.”

“Enquiries about Copyright and reproduction should be addressed to the Publications Officer, EFDA, Culham Science Centre, Abingdon, Oxon, OX14 3DB, UK.”

ABSTRACT.

The capabilities of the Joint European Torus (JET) Electron Cyclotron Emission (ECE) diagnostics have recently been extended with an upgrading of the heterodyne radiometer. The number of channels has been doubled to 96 channels, with a frequency separation corresponding to $< 1\text{cm}$ for JET magnetic field gradient, and with a frequency response of 1MHz. This enhancement has increased the radial coverage of the ECE electron temperature measurements in JET to approximately the full plasma column (limited at $R > 2.6\text{m}$ for the X-mode due to harmonic overlap) at almost all magnetic field values used at JET ($1.7\text{T} < B_T < 4\text{T}$), while maintaining the high sensitivity and spectral resolution of the previous system. In this paper an overview of the upgraded radiometer is presented along with some results showing its performance.

1. INTRODUCTION

The JET multi-channel heterodyne radiometer is one of the primary sources of electron temperature information in JET, particularly for those experiments where the time evolution of the temperature profile is of interest. The radiometer was constructed several years ago and during its lifetime it has been subjected to continuous development [1-2]. The most recent of which was devoted to enhance the radial resolution of the system by improving its spectral resolution, this involved halving the fixed frequency separation ($\sim 500\text{MHz}$) between the 48 channels and reducing the channel bandwidth (250MHz), but at the expense of reducing the total radial coverage. With the present upgrade, the number of the radiometer channels has been doubled to 96 to give improved radial coverage of the plasma, while maintaining the same spectral resolution of the previous system. This has been achieved by taking full advantage of the wide frequency coverage (69 – 139GHz) of the original instrument. A description of the upgraded system and some examples illustrating its performance are given in the following sections. Areas where further developments would be beneficial are identified.

2. RADIOMETER DESCRIPTION

The ECE radiation is collected from the tokamak low field side, perpendicular to the magnetic field along the major radius close to the equatorial mid-plane. The antenna is an oversize waveguide antenna ($50^\circ \times 65\text{mm}$) located at a height of 0.133m above the vacuum vessel mid-plane. Radiation from the plasma is transmitted [3] along a single long ($\sim 50\text{m}$) oversized waveguide (S-band/WG-10) to the radiometer and the detection system outside the biological protection wall. The heterodyne radiometer is shown schematically in Fig.1. By employing a series of non-polarizing wire grid and frequency selective beam-splitters the incident power is divided into six branches that transmit the signal to six independent heterodyne receivers. In each branch, wire grid polarizers together with waveguide switches allow either O- or X-mode radiation to be measured (for the first and second harmonic emission, respectively). After the polarization selection, the ECE radiation is down converted to an Intermediate Frequency (IF) by heterodyne mixing with a Local Oscillator (LO) and then amplified. The LO frequencies are chosen so that the 6 mixers give a continuous coverage

from 69 to 139GHz. The IF band range is 6 – 18GHz. The architecture of each of the six receivers is unchanged from that of the previous system [2].

The signals after the IF amplifiers are fed to IF switches, which allow four mixers with adjacent LO frequencies to be selected from the six available. A sub-set of four mixers provides sufficient radial coverage at almost all magnetic fields values used in JET ($1.7T < B_T < 4T$). In the IF stage, consisting of power dividers, IF filters and zero biased power detectors, the ECE radiation is split into 96 channels spread over 4 bands. Each band has 24 filters with 250MHz bandwidth, uniformly spaced ($\sim 500\text{MHz}$) across the IF band. In the previous system only two mixers were selected (a total of 48 channels grouped into two sets), limiting the radial coverage to $r/a \sim 0.2$ to 1. The output of the detector is amplified by a low noise video amplifier with a 1MHz bandwidth (110kHz in the previous system) and sent to either the standard data acquisition system or the fast acquisition system. The standard acquisition has video amplifiers with remotely programmable gain and bandwidth (up to 5kHz) and is used to routinely obtained T_e profile information. The amplifiers have a second output with a bandwidth of 400kHz for studying faster events. The fast acquisition, with sampling rate of 250kHz and 3s of data collection, provides information for MHD and fluctuations studies. A new fast data acquisition system has recently been installed that allows a large quantity of data (up to 6 Mbytes) to be taken at sample rates up to 1MHz [4]. The entire radiometer is designed to have a full remote control capability: the mixer selection, the polarisation to be observed by each band, the settings of the video main amplifier (gain and bandwidth) and the acquisition time window can be monitored and changed from the JET Control Room.

The total spatial resolution of the instrument is determined by a combination of different factors: (i) the size of the emitting volume that depends on the plasma parameters, the polarization and harmonic number of the observed radiation, (ii) the finite antenna pattern of the collection system [4] that broadens the volume contributing to the emission, and (iii) the spectral width of the detection system (IF bandwidth) that averages the contribution of different frequencies. The spatial resolution of the second harmonic X-mode emission is better (larger optical depth τ) than that of the first harmonic O-mode. The resolution improves for decreasing T_e and increasing n_e . For typical JET plasma parameters, the estimated radial resolution of individual channels is $\sim 2 - 5$ cm [6], while the separation between channels is $< 1\text{cm}$.

In principle, the high sensitivity of the radiometer makes absolute calibration with a low-temperature blackbody source possible. However, because of uncertainty about the long-term stability of its sensitivity, this technique has not been applied and it has been necessary to make use of cross-calibration against the absolutely calibrated Michelson interferometer. This instrument is capable of measuring the emission (X-mode) in the range of 90 – 450GHz with a frequency resolution of 10 GHz and a temporal resolution of 15ms. Since the two instruments have different spatial and temporal resolution, and use different lines of sight, care must be taken in the choice of conditions used for calibration, normally the stationary ohmic phase of a discharge. Recently, the magnetic field-ramp technique has been implemented to improve the ECE spectral calibration [7].

3. SOME MEASUREMENTS AND DISCUSSION

The upgraded radiometer has been operated routinely and with high reliability since September 2002. With the upgraded heterodyne radiometer, the radial coverage of the ECE measurements extends to almost the full plasma column (limited to $R > 2.6\text{m}$ in the case of X-mode radiation due to harmonic overlap) for a wide range of magnetic field values. This allows the simultaneous observation of edge and core electron temperatures as well as both high and low field side Internal Transport Barriers (ITB) with high spatial ($\sim 2\text{-}5\text{cm}$) and temporal (1 ms profile / 1 μs fluctuations) resolution. An example of the T_e profile of a high density ITB [8] measured by the radiometer is given in Fig.2. The figure also shows the T_e profile obtained by the LIDAR Thomson Scattering (TS) diagnostic [9] illustrating the good agreement generally obtained between these two independently calibrated diagnostics. As can be seen, the higher spatial resolution of the radiometer allows a better localization of the ITB position. The ECE data in JET are not routinely corrected for relativistic broadening (the effect is an inward shift of the emission origin), since the calculation of this correction is not straightforward and is usually small ($< 3\text{cm}$) [6]. In the figure, the radial profile of each diagnostic, which have different viewing directions, are mapped from their sightlines (and B space in the case of ECE) onto the magnetic axis using the EFIT equilibrium reconstruction code. The magnetic axis in this particular plasma configuration was displaced $\sim 0.35\text{m}$ above the mid-plane of the JET vacuum vessel and therefore the plasma centre was not accessible for the ECE measurements in this example.

For JET plasmas, the condition of large optical thickness for the second harmonic X-mode and the first harmonic O-mode is easily satisfied, even at frequencies corresponding to the edge plasma. This condition allows reliable T_e measurements in the edge pedestal [10]. This is illustrated in Fig. 3 which shows a comparison of the radiation temperature (T_{rad}) measured by ECE (second harmonic, X-mode) and T_e obtained with the edge Thomson Scattering diagnostic [11] in a discharge heated by 12MW of neutral beam injection (NBI). Both measurements agree for $R \leq 3.83\text{m}$ but diverge significantly in the outer region of the plasma. It is generally observed that there is a radial discrepancy in the profiles from the two diagnostics (the edge TS profile has to be shifted inwards by $< 50\text{mm}$), the reason for which is currently under investigation. Deficiencies in the flux surface mapping from the equilibrium code (which can have a significant effect on the position of the temperature profiles along the magnetic axis) may be sufficient to account for this discrepancy. The appearance of enhanced ECE radiation at or slightly outside the last closed flux surface is systematically observed in JET during H-mode and its appearance is correlated with the high edge T_e gradient. Similar observations have been reported in ASDEX-U [12]. Although it is clear that the origin of this enhanced radiation feature must be nonthermal (its intensity is too high to be produced by downshifted emission from the Maxwellian tail of the core plasma [13]), it is not fully understood which is the mechanism responsible of the generation of fast electron during NBI heating. Using the edge TS density and temperature profiles it is possible to infer the critical optical depth required for reliable edge ECE measurements. For plasmas with steep edge gradients, the transition from optically thick

to optically thin is very sharp, affecting only one or two radiometer channels (a few centimetres), hence the local minimum in the T_{rad} profile can be used to identify experimentally the radial position at which the plasma changes from optically thick to optically thin. In the case of the profiles shown in Fig.3, with a high T_e gradient, a critical optical depth of $\tau > 2$ is required for T_{rad} to equal T_e , however during the L-mode phase, good agreement between ECE and edge TS measurements is found for $\tau > 0.8$ (with $T_e > 300\text{eV}$ and $n_e > 4 \times 10^{18} \text{ m}^{-3}$). The ECE radiometer has been used in a wide range of physics studies in JET, such as: the dynamics of internal transport barriers [14], the diffusion of heat pulses induced by internal plasma instabilities or by external causes like ICRH heating [15], the dynamics of the edge pedestal during L-H transition or ELMS [16] or the spatial structure and temporal evolution of several kinds of fast temperature perturbations (e.g. sawteeth activity, collapse during pellet injection or plasma disruption). In addition, the electron temperature profile, and derived parameters such as its gradient, are available in real time for controlling the condition of the core plasma [17]. The use of real time control methods is expected to offer significant improvements in the performance of fusion plasma devices. While the performance of the radiometer is adequate for many applications, some improvements in hardware and calibration would be beneficial. A stable calibration is essential for real time applications. Periodic checks of drifts in calibration indicate that the reproducibility of the calibration factors on a short-term basis is better than 5%. However, in order to improve the long-term stability it would be necessary to implement a better control of the IF amplifier gain, which is temperature-sensitive. The applicability of the ECE measurements in high-density plasmas is restricted by the cutoff condition (internal reflection of the ECE radiation). This limitation could be partially alleviated by extending the spectral coverage of the radiometer, thus allowing X-mode second harmonic measurements at higher toroidal fields (currently central T_e data in Xmode is limited to $B_T < 2.5\text{T}$), the cut-off density for the second harmonic X-mode being twice that for the first harmonic O-mode. Additionally, microwave mixers with wider IF range up to 40GHz are now available, which permit a greater radial coverage with a single mixer. Finally, some effort is required to evaluate possible corrections to the cross-calibration with the X-mode Michelson when the radiometer is operated in O-mode.

ACKNOWLEDGEMENTS

The authors would like to acknowledge L. Porte and H. Oosterbeek for their contributions to the design and development of the original radiometer. The authors also would like to express their gratitude to the technical staff at JET, IPP and CIEMAT for their continuous support during the project. The first author would like to thank J. López for his invaluable assistance during the installation of the system. This work has been conducted under the European Fusion Development Agreement.

REFERENCES

- [1]. D. Bartlett *et al.*, Proc. of the 8th International Workshop on ECE and ECRH, Gut Ising, Germany (1992)
- [2]. D. Bartlett *et al.*, Proc. of the 9th International Workshop on ECE and ECRH, Borrego Springs, USA (1995)
- [3]. E. Baker *et al.*, Proc. of the 4th International Workshop on ECE and ECRH, Frascati, Italy (1984)
- [4]. N. Cruz *et al.*, 4th IAEA Topical Meeting on Control, Data Acquisition, and Remote Participation for Fusion Research, San Diego, USA, 2003
- [5]. N. A. Salmon, D.V. Bartlett and A. E. Costley, Proc. of the 6th International Workshop on ECE and ECRH, Oxford, UK (1987)
- [6]. V. Tribaldos, EFDA-JET Report, EFD-P (01) 44 (2001)
- [7]. P. Blanchard, C. Gowers and E. de la Luna, (this conference)
- [8]. D. Frigione *et al.*, Proc. of the 30th EPS Conference on Controlled Fusion and Plasma Physics, St. Petersburg, Russia (2003)
- [9]. C. Gowers *et al.*, Rev. Sci. Instrum. **66**, 471 (1995)
- [10]. L. Porte *et al.*, Proc. of the 10th International Workshop on ECE and ECRH, Ameland, Holland (1997). World Scientific Publications, 217(1997)
- [11]. C. Gowers *et al.*, Journal of Plasma and Fusion Research **76**, 874 (2000)
- [12]. A. G. Peeters *et al.*, Proc. of the 10th International Workshop on ECE and ECRH, Ameland, Holland (1997). World Scientific Publications, 403 (1997)
- [13]. D. V. Bartlett *et al.*, Proc. of the 19th EPS Conference on Controlled Fusion and Plasma Physics, Innsbruck, Austria (1992)
- [14]. X. Litaudon *et al.*, Nuclear Fusion **43**, 565 (2003)
- [15]. D. Van Eester *et al.*, Proc. of the 15th Topical Conference on Radio Frequency Power in Plasmas, Moran, USA (2003)
- [16]. S. Saarelma *et al.*, Plasma Physics and Controlled Fusion (submitted for publication)
- [17]. D. Mazon *et al.*, Plasma Physics and Controlled Fusion **44**, 1087 (2002)

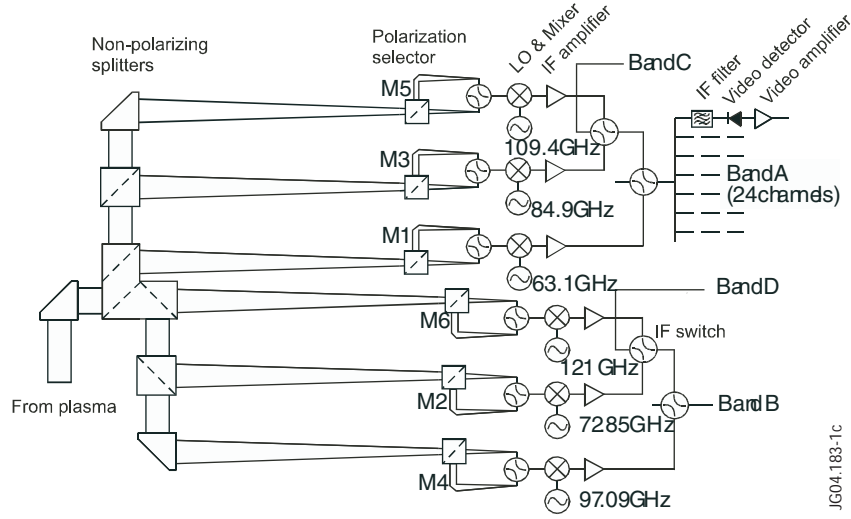


Figure 1. Schematic layout of the heterodyne receiver in JET.

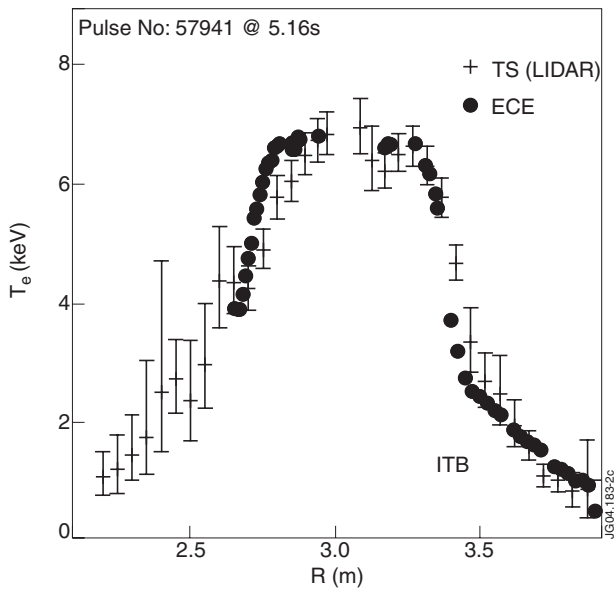


Figure 2. JET electron temperature profiles measured by ECE and Thomson scattering for a high density ITB discharge. The extended radial coverage of the upgraded radiometer allows simultaneous observation of both high and low field side ITBs. For this plasma configuration the radiometer line of sight passes 0.2 m below the plasma centre. (Plasma parameters: $B_T = 3.2T$, $I_P = 2MA$, $P_{NBI} = 8MW$, $PICRH = 6MW$, $T_e \sim T_i$, $n_e(0) = 6 \times 10^{19} m^{-3}$, close to the Greenwald value).

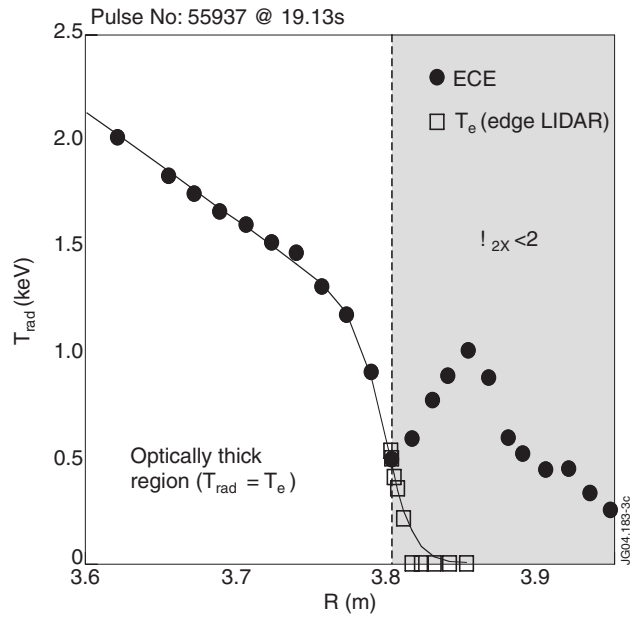


Figure 3. Comparison of the edge T_{rad} profile obtained from ECE (2nd harmonic, X-mode) and the T_e profile measured by edge LIDAR Thomson scattering during H-mode in JET (plasma parameters: $B_T = 2.4T$, $I_P = 2MA$, $P_{NBI} = 12MW$, $T_e(0) = 4keV$, $n_e(0) = 6 \times 10^{19} m^{-3}$). The curve is a fit to the data. Edge TS profile is shifted by $\sim 3cm$ to match the ECE profile. The local minimum that appears in the T_{rad} profile indicates the position in which the transition from optically thick to optically thin plasma occurs.